Conference - ISSS-7 -

Electronic Structure of Ni$_2$P(0001) Studied by Resonant Photoelectron Spectroscopy[*]

Shuhei Ishida, Yuichi Sugizaki, Takuya Nakamura, and Kazuyuki Edamoto[†]
Department of Chemistry, Rikkyo University, Toshima-ku, Tokyo 171-8501, Japan

Masaharu Matsunami
UVSOR Facility, Institute for Molecular Science, Okazaki 444-8585, Japan

Tetsuya Hajiri
Graduate School of Engineering, Nagoya University, Nagoya 464-8603, Japan

Shinichi Kimura
Graduate School of Frontier Biosciences, Osaka University, Suita, 565-0871, Japan

The electronic structure of Ni$_2$P(0001) has been investigated by photoelectron spectroscopy (PES) utilizing synchrotron radiation. A Ni $3d$–P $3p$ hybrid band was observed at 1-5 eV, and the band had peaks at 1.5 eV and 3.4 eV together with a shoulder around 2.4 eV. The resonant PES study showed that the Ni 3d component was included in the whole binding energy region of the band. The change in the surface electronic structure of Ni$_2$P(0001) induced by the segregation of P atoms was investigated by annealing temperature-dependent measurements of PES, and it was found that the change proceeded via following two steps: the segregation of P atoms proceeded at about 200°C, and the bonding between surface Ni atoms and segregated P atoms was facilitated at > 300°C. The bonding between Ni and P atoms induced substantial stabilization of Ni $3d$ levels, which is contrary to the case of Fe$_2$P(0001) where the segregation of P atoms induced little change in DOS of Fe 3d levels. [DOI: 10.1380/ejssnt.2015.93]

I. INTRODUCTION

The surface properties of transition metal phosphides (TMPs) have attracted much attention because these have been found to have high catalytic activities for hydroprocessing reactions such as hydrodesulfurization (HDS) and hydrodenitrogenation (HDN) for petroleum fuels [1,2]. Of all TMPs studied thus far, it has been found that Ni$_2$P has the highest catalytic performance for these reactions [1,2]; the HDS conversion for dibenzothiophene is nearly 100% [1]. The conversion rate is substantially higher than that of currently used sulfide-based catalysts, and Ni$_2$P is a promising material as the catalyst of HDS in the next generation. On the other hand, the catalytic activity of Fe$_2$P presents striking contrast to that of Ni$_2$P; the HDS conversion for dibenzothiophene is only several % [1]. It is a wonder that the catalytic activities of Ni$_2$P and Fe$_2$P are much different from each other, because the electronic structures of these materials are thought to be similar with each other; these are typical metal-rich phosphides and both crystals are expected to have metallic electronic structures [1]. In addition, Fe$_2$P and Ni$_2$P crystals belong to the same space group (P$\bar{6}$2m) and both crystals consist of two types of atomic layers with the stoichiometry of M$_3$P and M$_3$P$_2$ (M = Ni, Fe) which are stacking alternatively along the [0001] direction [3]. One of the possible reasons for the difference in catalytic activity is that the surface electronic structures of these materials, especially those of active metal sites, are different with each other.

Therefore, in order to elucidate the origin of the high catalytic performance of TMPs, it is useful to explore the difference in the surface electronic structures of Fe$_2$P and Ni$_2$P.

The characterization of a Ni$_2$P single-crystal surface has been mainly attempted for a (0001) surface [3-12]. An ideal (0001) surface should be terminated with either a Ni$_3$P- or a Ni$_3$P$_2$-layer, and theoretical studies by Liu et al. using density functional theory (DFT) calculations have predicted that the Ni$_3$P$_2$-terminated surface is more stable than the Ni$_3$P-terminated surface by 2.75 eV/unit cell [4,5]. Li and Hu made first-principles calculations of the electronic structure of Ni$_2$P(0001), and also concluded that the Ni$_3$P$_2$-terminated surface is more stable [6]. However, previous structural analyses using low-energy electron diffraction (LEED) and scanning tunneling microscopy (STM) have revealed that, in addition to a (1×1) termination, several reconstructed phases such as $3/2 \times 3/2$ and $\sqrt{3} \times \sqrt{3}$ R30° are also realized on the surface [7-9]. Furthermore, Hernandez et al. made a dynamical LEED study for the (0001) surface, and proposed that even the (1 × 1) surface is not an ideal surface and should be a Ni$_3$P$_2$-terminated surface on which P atoms sit above threefold sites of three Ni atoms (P-terminated Ni$_3$P$_2$-surface) [10]. As for the electronic structure, our group performed an angle-resolved photoemission spectroscopy (ARPES) study on Ni$_2$P(0001) and found that the normal-emission spectra consist of a Ni $3d$–P $3p$ hybrid band (main band) and a satellite at 0-4 eV and 8 eV, respectively [11,12]. As for Fe$_2$P surfaces, our group recently performed an angle-integrated PES study for Fe$_2$P(0001), and found that a Fe $3d$–P $3p$ hybrid band was formed at 0-3 eV, and the band consisted of a peak at 0.2 eV and a shoulder at 2.0 eV [13]. The band seemed to be formed in the lower binding energy side with respect

_____

to the Ni 3d–P 3p band in Ni$_2$P [13], suggesting that the stabilization of metal sites owing to the bonding with P atoms is ineffective in Fe$_2$P. The stabilization of metal sites is thought to be important to prevent deactivation of the surface induced by accumulation of S atoms on active metal sites during HDS reactions. In this paper, we report the results of an angle integrated PES study on Ni$_2$P(0001) using the same experimental set-up as that in our previous study of Fe$_2$P(0001) [13]. The possible origin of the difference in the catalytic activities of Ni$_2$P and Fe$_2$P will be discussed.

II.   EXPERIMENTAL

A Ni$_2$P single-crystal was grown by Dr. S. Otani of the National Institute for Materials Science using a floating zone method. The crystal was cut at an orientation of (0001) by spark erosion into a disk of 1 mm thickness, and the surface was polished mechanically to a mirror finish. The surface was cleaned in a vacuum chamber by several cycles of Ar$^+$ ion sputtering (1-3 kV, 30 min) and annealing at 600°C for 30 min. The clean surface prepared by this procedure gave a hexagonal (1 × 1) LEED pattern, and no impurity was observed within the detection limit of Auger electron spectroscopy (AES). The PES measurements were performed at BL-5U of the UVSOR Facility, Institute for Molecular Science, using an electron energy analyzer of MBS-Toyama A-1. The acceptance angle of the analyzer was ±18°. The total experimental resolution was estimated from the Fermi edge in the spectra of Ni$_2$P(0001) measured at room temperature, and was estimated to be 110 meV at $h\nu = 60$ eV, which includes thermal broadening contribution to the width at 300 K. The spectra presented below were normalized by the photocurrent of a gold mesh which was inserted at the entrance of the analysis chamber. The incidence angle of the light was 45° from the surface normal direction, and the analyzer axis was parallel to the surface normal direction. The base pressure in the vacuum system was 1.8×10^{-8} Pa.

III.   RESULTS AND DISCUSSIONS

The PES spectra of Ni$_2$P(0001) were measured at various photon energies of $h\nu = 46 - 80$ eV, and the spectra measured at $h\nu = 62 - 74$ eV are shown in Fig. 1. An intense band is observed at 1-5 eV, and the band has peaks at 1.5 eV and 3.4 eV together with a shoulder around 2.4 eV independent of photon energy. The peaks are called peak A and peak B, respectively, and the shoulder is called peak S, hereafter. The peak B has not been clearly observed in previous ARPES studies [11, 12], and the reason will be discussed later. The band observed at 1-5 eV is ascribed to a Ni 3d–P 3p hybrid band (main band) [4-6]. Though a clear cut-off is observed at the Fermi level (E$_F$) independent of $h\nu$, the density of states (DOS) around E$_F$ is suppressed due to the hybridization of Ni 3d levels with P 3p levels forming a pseudo gap. A band is also observed at 8 eV, and previous resonant PES studies showed that the peak is ascribed to a satellite which is associated with
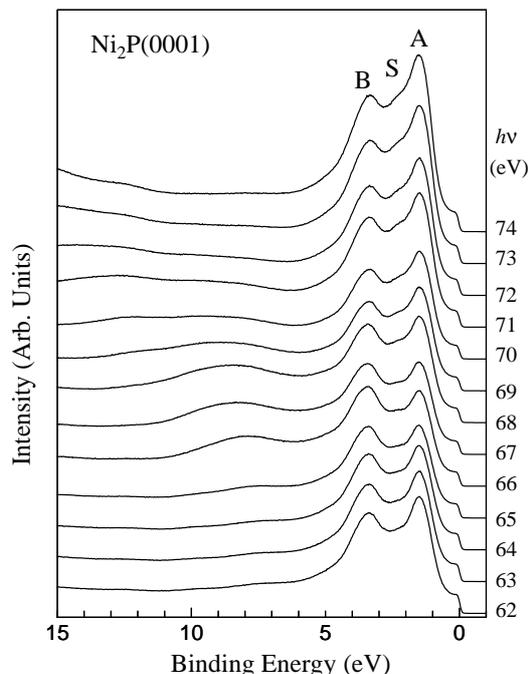
FIG. 1. PES spectra of Ni$_2$P(0001) measured at various photon energies of 62-74 eV.

the Ni 3d photoemission leading to a two-hole bound final state [11,12]. An additional broad band, which shifts to the higher binding energy side with increasing $h\nu$, is observed at $h\nu > 69$ eV, and the band is ascribed to a Ni M$_{23}$VV Auger peak [11,12].

The PES spectra of Ni$_2$P(0001) after Ar$^+$ ion sputtering (3 kV, 10 min) and of the surface subsequently annealed at elevating temperatures are shown in Fig. 2. The spectra are measured at $h\nu = 60$ eV. The spectrum of the surface after annealing at 600°C (the topmost spectrum) is the same as that before sputtering. When the surface is sputtered, the peak A slightly shifts to the lower binding energy side by 0.2 eV and the peak B is almost suppressed, and the overall band intensity is enhanced as compared with those in the spectra of the surface before sputtering. As the Ni$_2$P(0001) surface is subjected to Ar$^+$ ion sputtering, it has been proved that P atoms in the surface region are selectively removed [3]. The photoionization cross section of Ni 3d (9 Mb) is much higher than that of P 3p (0.5 Mb) at $h\nu = 60$ eV [14], and therefore the enhancement of the band intensity is explained to be due to the increase of the component of Ni 3d electrons in the valence band due to the removal of P atoms in the surface region, because the formation of the Ni 3d–P 3p bond should result in the partial donation of Ni 3d electrons to the P 3p levels [11,12]. As the surface is annealed at 150-300°C, the band is decreased in intensity though the spectral profile is nearly unchanged. A previous XPS study by Kanama *et al.* showed that the segregation of bulk P atoms toward the Ni$_2$P(0001) surface proceeds by annealing the sputtered surface at around 200°C [3], and thus the decrease of the band intensity by annealing at 150-300°C is ascribed to the increase of the component of P 3p electrons in the valence band due to the surface segregation of P atoms. The spectrum is substantially changed by annealing at

600°C; the peak A shifts to the higher binding energy side and the peak B grows, and overall band intensity is further decreased. Essentially the same result has been obtained by Kanama *et al.* using He II UPS [3], though the peak B is more clearly observed in this study. Though the XPS Ni/P intensity ratio is nearly constant by annealing at higher than 200°C [3], the substantial change in the surface electronic structure proceeds by annealing at > 300°C. Therefore, we propose that the change in the surface electronic structure of Ni₂P(0001) induced by P segregation proceeds via following two steps; the segregation of bulk P atoms toward the surface proceeds by annealing at around 200°C, and the bonding between Ni and segregated P atoms in the surface region is facilitated by annealing at > 300°C. The state of the segregated P atoms in the first step is unknown at present. The spectral shape of the valence band is not changed by the P segregation, and thus one of the possible situations is that the segregated P atoms occupy some interstitial sites around the surface, which is thought to give little effect on the spectral shape due to the low photoionization cross section of P states. However, since the overall valence band intensity is decreased also in the first step, partial change transfer from Ni atoms to segregated P atoms may occur in this stage. A normal-emission spectrum of Ni₂P(0001) at $h\nu = 60$ eV measured in our previous ARPES studies [11,12] is shown as a dotted line in Fig. 2. Though the spectrum was measured in an angle-resolved mode, the spectral profile was nearly independent of $h\nu$ and detection angles (θ_d) [11,12], unlike the case of the ARPES study of Ni₂P(10$\bar{1}$0) in which the θ_d-dependent dispersion was observed [15]. The origin of the lack of the dispersion of ARPES from Ni₂P(0001) is unknown, and one of possible reasons proposed in Refs. [11] and [12] was that the spectra reflect three dimensional DOS. However, the spectral profile is not the same as that obtained in the present study; the valence band seems to consist of peaks A and S, while the peak B is not observed, and the peak A locates in the lower binding energy side with respect to that observed in the present work. This is thought to be due to the difference in the annealing condition; the surface is annealed at 600°C for 10 min in our previous works [11,12] while the surface was annealed at 600°C for prolonged time (30 min) in the present work. The formation of Ni–P bond should be a slow process, and the peak B is thought to arise from the hybridization of the 3d levels of surface Ni atoms with the 3p levels of segregated P atoms. The segregation behavior of P atoms was also studied for Ni₂P(10$\bar{1}$0), and it was proposed that the P atoms in the surface region were selectively removed by Ar⁺ ion sputtering, and that the annealing of the sputtered surface induced P segregation which proceeded at 260-330°C [16-18]. The segregation behavior is qualitatively the same as that of Ni₂P(0001), though the segregation occurs at relatively low temperature region for Ni₂P(0001).

The integrated intensities of the main band in the spectra of Ni₂P(0001) are plotted as a function of $h\nu$ in Fig. 3(a) (open circles). The background drawn by the Shirley procedure was subtracted from each raw data before integration. In Fig. 3(a), the integrated intensities of the satellite are also plotted as filled circles. The background approximated to be a polynominal function was subtracted from each raw data to estimate the satellite
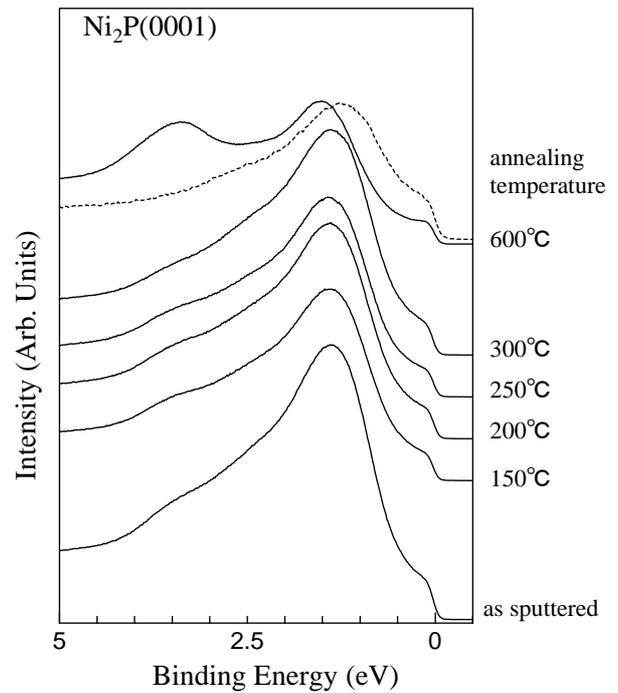
FIG. 2. PES spectra of Ni₂P(0001) after Ar⁺ ion sputtering (3 kV, 10 min), and of the surface subsequently annealed at elevating temperatures ($h\nu = 60$ eV). A normal-emission spectrum of Ni₂P(0001) measured in a previous study [11] ($h\nu = 60$ eV) is shown as a dotted line.

intensity. The satellite is overlapping with a Ni M₂₃VV Auger peak around $h\nu = 68$ eV, and the sum of the intensities of the satellite and the Auger peak is plotted at $h\nu \geqq 68$ eV. The $h\nu$-dependence of the satellite intensity is identical to that reported in previous resonant PES studies; the intensity is maximized around the Ni 3p photoexcitation threshold (~ 70 eV) [11,12]. The intensity maximum is interpreted as caused through the resonance arising from the interference between a direct Ni 3d photoemission process and a process induced by the Ni 3$p \rightarrow 3d$ photoexcitation followed by a Ni 3d electron emission through an Auger process [11,12]. The latter process leads to a final state with two correlated d holes, and thus the satellite is associated with the Ni 3d photoemission leading to the two-hole bound final state. On the other hand, the $h\nu$-dependence of the main band intensity is characterized by the existence of a minimum around the Ni 3p photoexcitation threshold ($h\nu = 67$ eV). The existence of the minimum of the main band intensity around the Ni 3p photoexcitation threshold was also observed in the previous resonant PES studies [11,12], though the dip structure is more prominently observed in the present study. The intensity minimum was explained to be caused through the same resonance process as that for satellite; the super-Coster-Kronig decay of the 3$p \rightarrow$ 3d excited state leads to the two-hole final state, and the satellite and the main band are resonated when the final state is localized and delocalized, respectively [19,20]. In this case, the $h\nu$-dependence of the main band intensity is simulated to be a Fano line-shape with a minimum around the 3p photoexcitation threshold [19,20]. On the other

hand, Hüfner gave a more simple explanation that the intensity minimum is originated from the fact that many of the photons impinging on the Ni atoms are used for the $3p \rightarrow 3d$ excitation rather than the direct $3d$ photoemission around the Ni $3p$ photoexcitation threshold [21]. In either case, the appearance of the dip around 67 eV is characteristic of the Ni $3d$ photoemission. The heights of peaks A, B and S in each spectrum after subtracting the Shirley background are plotted as a function of $h\nu$ in the inset of Fig. 3(a). The intensities of all three peaks show nearly the same $h\nu$-dependence and are minimized around 67 eV, indicating that the Ni $3d$ components are included in the whole valence band region. Though the peak B should arise from the hybridization between the $3d$ levels of surface Ni atoms and the $3p$ levels of the segregation of P atoms, the resonant PES study shows that the state includes substantial contribution of Ni $3d$ components as in the case of peaks A and S.

The valence band spectra of $Fe_2P(0001)$ also consist of a main band and satellites [13], and the PES spectra measured at $h\nu = 49$ and 53 eV are shown in the inset of Fig. 3(b). A Fe $3d$–P $3p$ hybrid band (main band) is observed at 0-3 eV, and satellites are observed at 4.5 and 7 eV. The origin of the two-peak structure of the satellite is unknown at present. In Fig. 3(b), the integrated intensities of the main band (open circles) and those of the sum of satellites (filled circles) in the PES spectra of $Fe_2P(0001)$ are plotted as a function of $h\nu$ [13]. At $h\nu > 55$ eV, a Fe MVV Auger emission peak is overlapping with the satellites, and the intensity at $h\nu > 55$ eV (filled circles) is the sum of the satellites and Auger peak intensities. As in the case of $Ni_2P(0001)$, the satellite intensity shows a maximum and the main band intensity shows a minimum around the Fe $3p$ photoexcitation threshold (54 eV). The resonant behavior of the photoemission from $Fe_2P(0001)$ is similar to that from $Ni_2P(0001)$. However, the comparison of the plots in Figs. 3(a) and 3(b) shows that the resonant enhancement of the satellite intensity is more intense for $Fe_2P(0001)$ than that for $Ni_2P(0001)$; the intensity of the satellite at resonance maximum relative to that in the off-resonance region is 21 for $Fe_2P(0001)$ while that is 10 for $Ni_2P(0001)$. It has been revealed that the intensity of the resonance depends on the number of $3d$ holes [22,23], which qualitatively explains the difference in the resonance intensities of $Fe_2P(0001)$ and $Ni_2P(0001)$. Chandesris *et al.* estimated the intensity of the resonance of PES of several $3d$ metals by the use of a parameter defined as the satellite intensity relative to the main band intensity (I_{sat}/I_{main}) at resonance, and reported that the resonance intensity of Fe is about 2.8 times of that of Ni [22]. However, the resonance intensity (I_{sat}/I_{main}) is about 0.2 for $Ni_2P(0001)$ while that is 9.5 for $Fe_2P(0001)$, and thus the resonance intensity of $Fe_2P(0001)$ is about 48 times of that of $Ni_2P(0001)$, indicating that the ratio of the resonance intensity of Fe $3d$ relative to that of Ni $3d$ is enhanced by the formation of phosphides. We think that this is mainly due to the difference in the valence electronic structures formed through the metal–P bonding. For Fe_2P, a Fe $3p_{3/2}$ peak was observed at 53 eV [13], and the resonance maximum is observed at $h\nu = 54$ eV. Therefore, the resonance is caused through the excitation of Fe $3p$ electrons to the unoccupied states just above E_F. The valence band spectra
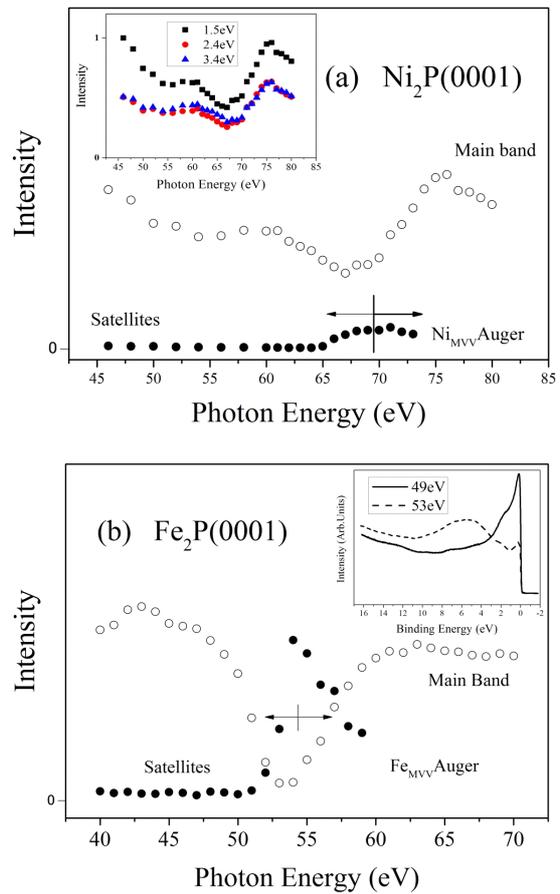
FIG. 3. (a) Integrated intensities of the main band (open circles) and the satellite band (filled circles) in PES spectra of $Ni_2P(0001)$ as a function of $h\nu$. The latter plots correspond to the sum of the intensities of the satellite peak and the intensities of an Auger peak at $h\nu \geqq 68$ eV. The heights of peaks A, B and S are plotted as a function of $h\nu$ in the inset. (b) Integrated intensities of the main band (open circles) and the satellite band (filled circles) in PES spectra of $Fe_2P(0001)$ as a function of $h\nu$. The latter plots correspond to the sum of the intensities of the satellite peak and the intensities of an Auger peak at $h\nu \geqq 55$ eV. PES spectra of $Fe_2P(0001)$ measured at $h\nu = 49$ and 53 eV are shown in the inset.

of $Fe_2P(0001)$ is characterized by the existence of a sharp peak just below E_F as shown in the inset of Fig. 3(b) and Fig. 4, and thus the band with high DOS is formed around E_F, which implies that the Fe $3p \rightarrow 3d$ excitation occurs with high photoabsorption intensity. For Ni_2P, a Ni $3p_{3/2}$ peak was observed at 67 eV [11,12], and the resonance maximum is observed at ~ 70 eV (Fig. 4(a)), suggesting that the final state of the Ni $3p \rightarrow 3d$ excitation locates at slightly above E_F. In the case of Ni_2P, DOS around E_F is suppressed due to the hybridization of Ni $3d$ levels with P $3p$ levels forming a pseudo gap (Fig. 1). Therefore, the Ni $3p \rightarrow 3d$ photoexcitation probability becomes relatively low as compared with the case of Fe_2P. The difference in the electronic structures of $Fe_2P(0001)$ and $Ni_2P(0001)$ will be also discussed in the next paragraph. The other possible origin of the difference in resonance intensities is the difference in the charged states of metal sites. Previous core-level PES studies showed that the $2p_{3/2}$ level

of bulk P atoms locate at 129.3 eV for $Fe_2P(0001)$ [13] and at 129.6 eV for $Ni_2P(0001)$ [11,12], while the $2p_{3/2}$ level of simple substance of P has been observed at 130.2-130.9 eV [24]. Therefore, both of the P atoms in Fe_2P and those in Ni_2P are negatively charged, and core-level PES studies show that the P atoms in Fe_2P is more negative than those in Ni_2P. Therefore, the increase of $3d$ holes due to the formation of phosphide is more prominent in Fe_2P, which should be one of the reasons of the higher resonance intensity for the photoemission from Fe_2P.

In order to compare the electronic structures of $Ni_2P(0001)$ and $Fe_2P(0001)$, the valence band spectra of these surfaces measured in the off-resonance region ($h\nu = 60$ and 49 eV, respectively) are shown in Fig. 4 (solid lines). The photoionization cross sections of Ni $3d$ (9 Mb) and Fe $3d$ (10 Mb) are much higher than that of P $3p$ (0.5 Mb) at these photon energies [14], and thus the spectra mostly reflect DOS of metal $3d$ components. Both of Ni and Fe metals are known to have large DOS at E_F, because the Fermi level intersects the $3d$ bands [22,23]. However, the valence band of $Ni_2P(0001)$ is observed at 1-5 eV and DOS around E_F is relatively small, indicating that the Ni $3d$ levels are effectively stabilized through the hybridization with P $3p$ levels. On the other hand, the spectrum of $Fe_2P(0001)$ has large emission around E_F and the spectral shape is similar to that of a Fe metal [22], and thus the Fe $3d$ levels are not effectively stabilized in Fe_2P. The electronic states around E_F should play a crucial role in surface reactions, and Fe atoms in Fe_2P should remain reactive in spite of bonding with P atoms. In Fig. 4, the spectra of these surfaces after Ar^+ ion sputtering are also shown as dotted lines. The sputtering of $Ni_2P(0001)$ (3 kV, 10 min) induces a substantial spectral change; the band is totally shifted to the lower binding energy side and the intensity is enhanced, and the spectrum reversibly returns back to original one by annealing the surface. These results mean that the $3d$ levels of surface Ni atoms are stabilized through the bonding with segregated P atoms after annealing. On the other hand, the sputtering of $Fe_2P(0001)$ induces little change in the PES spectrum (Fig. 4). Though the sputtering condition is mild (1 kV, 5 min) relative to that for $Ni_2P(0001)$, it has been confirmed by P $2p$ core-level measurements that P atoms in the surface region are selectively removed by this sputtering condition [13]. Therefore, it is concluded that the stabilization of the surface Fe atoms due to the bonding with the segregated P atoms is not effective on $Fe_2P(0001)$. The stabilization of the $3d$ levels of active metal sites is denoted as a "ligand effect" [4], and is predicted to be important to maintain the activity of TMP catalysts in HDS reactions through the prevention of the accumulation of S atoms on the active metal sites. The present study suggests that the ligand effect is effective on $Ni_2P(0001)$, while that is not effective on $Fe_2P(0001)$, which should be one of the reasons for the difference in the catalytic activities of Ni_2P and Fe_2P for HDS.

FIG. 4. PES spectra of $Ni_2P(0001)$ and $Fe_2P(0001)$ clean surfaces (solid lines) and of the surfaces after slight Ar^+ ion sputtering (3 kV for 10 min and 1 kV for 5min, respectively) (dotted lines). The spectra are measured at $h\nu = 60$ eV and 49 eV, respectively.

band) and the satellite were observed at 1-5 eV and at 8 eV, respectively. The main band consisted of peaks at 1.5 eV and 3.4 eV together with a shoulder around 2.4 eV. The peak at 3.4 eV was formed through the bonding between surface Ni atoms and segregated P atoms, while the resonant PES study showed that the intensities of all three peaks were minimized around the Ni $3p$ photoexcitation threshold, indicating that substantial contributions of Ni $3d$ levels are included in all three peaks. The change in the surface electronic structure of $Ni_2P(0001)$ induced by the segregation of P atoms was investigated by annealing temperature-dependent measurements of PES, and it was found that the substantial change of the surface electronic structure was induced by annealing at $> 300°C$, while the P segregation occurred at about 200°C. These results suggest that the change proceeds via following two steps: the segregation of P atoms proceeds at about 200°C, and the bonding between surface Ni atoms and segregated P atoms is facilitated at $> 300°C$. The bonding between Ni and P atoms induced substantial stabilization of Ni $3d$ levels, which is contrary to the case of $Fe_2P(0001)$ where the segregation of P atoms induced little change in DOS of Fe $3d$ levels.

IV.   CONCLUSION

The valence electronic structure of $Ni_2P(0001)$ was investigated by photoelectron spectroscopy (PES) utilizing synchrotron radiation. The Ni $3d$–P $3p$ hybrid band (main

[1] S. T. Oyama, J. Catal. **216**, 343 (2003).

[2] S. T. Oyama, T. Gott, H. Zhao, and Y.-K. Lee, Catal. Today **143**, 94 (2009).

[3] D. Kanama, S. T. Oyama, S. Otani, and D. F. Cox, Surf. Sci. **552**, 8 (2004).

[4] P. Liu, J. A. Rodriguez, T. Asakura, J. Gomes, and K. Nakamura, J. Phys. Chem. B **109**, 4575 (2005).

[5] P. Liu and J. Rodriguez, J. Am. Chem. Soc. **127**, 14871 (2005).

[6] Q. Li and X. Hu, Phys. Rev. B **74**, 035414 (2006).

[7] M. G. Moula, S. Suzuki, W. J. Chun, S. Otani, S. T. Oyama, and K. Asakura, Chem. Lett. **35**, 90 (2006).

[8] M. G. Moula, S. Suzuki, W. J. Chun, S. Otani, S. T. Oyama, and K. Asakura, Surf. Interface Anal. **38**, 1611 (2006).

[9] K. Kinoshita, G. H. Simon, T. König, M. Heyde, H. J. Freund, Y. Nakagawa, S. Suzuki, W. J. Chun, S. T. Oyama, S. Otani, and K. Asakura, Jpn. J. Appl. Phys, **47**, 6088 (2008).

[10] A. B. Hernandez, H. Ariga, S. Takakusagi, K. Kinoshita, S. Suzuki, S. Otani, S. T. Oyama, and K. Asakura, Chem. Phys. Lett. **513**, 48 (2011).

[11] K. Edamoto, Y. Nakadai, H. Inomata, K. Ozawa, and S. Otani, Solid State Commun. **148**, 135 (2008).

[12] K. Edamoto, H. Inomata, T. Shimada, K. Ozawa, and S. Otani, e-J. Surf. Sci. Nanotech. **7**, 1 (2009).

[13] Y. Sugizaki, S. Ishida, Y. Kakefuda, K. Edamoto, M. Matsunami, T. Hajiri, and S. Kimura, Surf. Sci. **624**, 21 (2014).

[14] J. J. Yeh and I. Lindau, Atomic Data and Nuclear Data Tables **32**, 1 (1985).

[15] K. Edamoto, H. Inomata, K. Ozawa, Y. Nakagawa, K. Asakura, and S. Otani, Solid State Commun. **150**, 1120 (2010).

[16] S. Imanishi, S. Munakata, Y. Kakefuda, K. Edamoto, and K. Ozawa, e-J. Surf. Sci. Nanotech. **10**, 45 (2012).

[17] K. Edamoto, Appl. Surf. Sci. **269**, 7 (2013).

[18] K. Edamoto, S. Imanishi, S. Masuda, Y. Kakefuda, and K. Ozawa, e-J. Surf. Sci. Nanotech. **12**, 175 (2014).

[19] L. C. Davis and L. A. Feldkamp, Phys. Rev. B **23**, 6239 (1981).

[20] L. C. Davis, J. Appl. Phys. **59**, R25 (1986).

[21] S. Hüfner, *Photoelectron Spectroscopy* (Springer, Berlin, 1995).

[22] D. Chandesris, J. Lecante, and Y. Petroff, Phys. Rev. B **27**, 2630 (1983).

[23] M. R. Thuler, R. L. Benbow, and Z. Hurych, Phys. Rev. B **27**, 2082 (1983).

[24] A. M. Puziy, O. I. Poddubnaya, and A. M. Ziatdinov, Appl. Surf. Sci. **252**, 8036 (2006).